Neuron 51, 575–586, September 7, 2006 ©2006 Elsevier Inc. DOI 10.1016/j.neuron.2006.07.012

RGS2 Determines Short-Term Synaptic Plasticity in Hippocampal Neurons by Regulating $G_{i/o}$-Mediated Inhibition of Presynaptic Ca^{2+} Channels

Jing Han,[1] Melanie D. Mark,[1] Xiang Li,[1] Mian Xie,[1] Sayumi Waka,[1] Jens Rettig,[2] and Stefan Herlitze[1,*]
[1] Department of Neurosciences
Case Western Reserve University
School of Medicine
Room E 604
10900 Euclid Avenue
Cleveland, Ohio 44106
[2] Department of Physiology
Saarland University
66421 Homburg
Germany

Summary

RGS2, one of the small members of the regulator of G protein signaling (RGS) family, is highly expressed in brain and regulates $G_{i/o}$ as well as G_q-coupled receptor pathways. RGS2 modulates anxiety, aggression, and blood pressure in mice, suggesting that RGS2 regulates synaptic circuits underlying animal physiology and behavior. How RGS2 in brain influences synaptic activity is unknown. We therefore analyzed the synaptic function of RGS2 in hippocampal neurons by comparing electrophysiological recordings from RGS2 knockout and wild-type mice. Our study provides a general mechanism of the action of the RGS family containing RGS2 by demonstrating that RGS2 increases synaptic vesicle release by downregulating the $G_{i/o}$-mediated presynaptic Ca^{2+} channel inhibition and therefore provides an explanation of how regulation of RGS2 expression can modulate the function of neuronal circuits underlying behavior.

Introduction

G protein signaling couples extracellular signals with intracellular effectors. G protein coupled receptor (GPCR) activation via neurotransmitters initiates the exchange of GDP for GTP on the Gα subunit, allowing the dissociation of the Gβγ subunit and enabling it to interact with different effectors, such as ion channels. The hydrolysis of GTP to GDP on the Gα subunit leads to the reassociation of the Gβγ dimer with the Gα subunit and termination of the signal (Hamm, 1998). The termination of the G protein signal is accelerated by a superfamily of GTPase accelerating proteins (GAPs) known as RGS proteins. Besides their function as GAPs for the termination of the G protein signals, RGS proteins can act as effector antagonists by blocking the G_q pathway (De Vries et al., 2000).

GPCRs are found at presynaptic and postsynaptic terminals and are involved in the regulation of neuronal excitability. RGS proteins accelerate both the onset and decay of G protein-mediated signals (Herlitze et al., 1999; Zerangue and Jan, 1998). This implies that RGS is essential for precise physiological signaling events such as synaptic transmission in the central nervous system, which involves G protein-coupled receptor cascades and ion channels. In addition, several studies demonstrate the modulation of presynaptic Ca^{2+} channels of the N-, P/Q- and R-type (Jarvis and Zamponi, 2001) in heterologous expression systems. These studies reveal that RGS accelerates the onset and offset of transmitter-mediated inhibition of presynaptic Ca^{2+} channels and also point to a role of RGS in altering the amount of inhibition for the presynaptic Ca^{2+} channels.

Among the RGS family, RGS2 plays a prominent role in the brain. A regulatory role of RGS2 in synaptic transmission and plasticity was suggested when RGS2 knockout mice revealed a decrease in synaptic activity in hippocampal CA1 neurons probably correlated with increased anxiety in the mice (Oliveira-Dos-Santos et al., 2000). Genetic dissection of a behavioral quantitative trait locus also revealed that RGS2 is a modulator of anxiety in mice (Yalcin et al., 2004). RGS2 expression has been shown to be rapidly upregulated in various brain regions, such as the hippocampus, by excitatory stimuli (Burchett et al., 1998; Ingi et al., 1998), and it is therefore likely that regulation of RGS2 protein levels in neurons regulates synaptic output and behavior.

Thus, the abundance of GPCRs at presynaptic terminals and their involvement in presynaptic Ca^{2+} channel inhibition, the functional interaction between RGS2 and presynaptic Ca^{2+} channels in heterologous expression systems as well as neurons, and the fact that *RGS2*$^{-/-}$ mice reveal reduced synaptic activity accompanied with behavioral changes suggest that RGS2 acts at the presynaptic terminal. However, direct evidence for this hypothesis is still lacking. We therefore examined the effect of RGS2 on synaptic transmission by exogenously expressing RGS2 in cultured hippocampal neurons and comparing the results with recordings from *RGS2*$^{-/-}$ neurons. Our data suggest that RGS2 regulates synaptic output via modulation of basal G protein activity of the $G_{i/o}$, but not the G_q, pathway at the presynaptic terminal. This result is surprising, given the fact that RGS2 has been described for its high affinity for the G_q, but not the $G_{i/o}$, pathway.

Results

RGS2 Is Endogenously Expressed in Cultured Hippocampal Neurons and Colocalizes with the Synaptic Marker Synaptobrevin-2

The goal of this study was to understand if and how RGS2 regulates synaptic transmission. A well-established model system for performing such experiments is to compare defined synaptic parameters between knockout and wild-type autaptic hippocampal neurons and to rescue the effects observed in knockout cultures by exogenously expressing the wild-type protein (see for example Bekkers and Stevens, 1991; Calakos et al., 2004; Rhee et al., 2002). Since no specific antibodies are commercially available to detect RGS2 protein (see Figure S1 in the Supplemental Data), we performed

*Correspondence: sxh106@cwru.edu

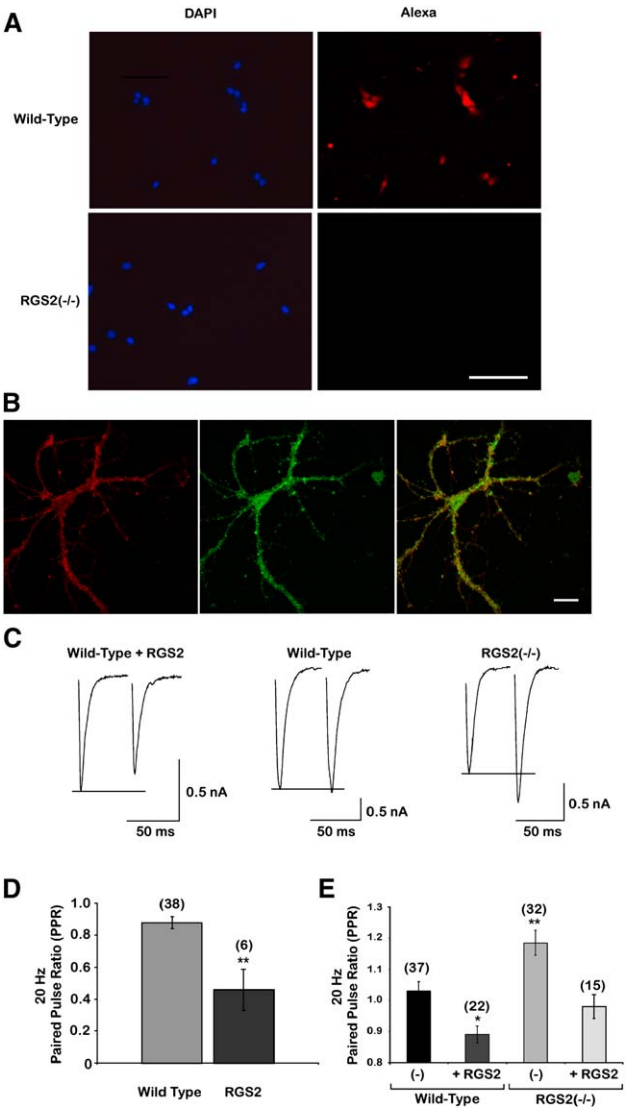

Figure 1. RGS2 Expressed in Hippocampal Neurons Targets to Synaptic Sites and Regulates Short-Term Synaptic Plasticity

(A) RGS2 mRNA is expressed in neurons from wild-type hippocampal cultures, but not in cultures from *RGS2*$^{-/-}$ mice. In situ hybridization of neurons from low-density hippocampal cultures of wild-type mice (upper panel) and *RGS2*$^{-/-}$ mice (lower panel). (Left) Nuclei of neurons were visualized with DAPI staining. RGS2 mRNA was detected with a DIG-labeled probe and visualized with an Alexa546-coupled anti-DIG antibody. Scale bar, 10 μm.

(B) Exogenously expressed RGS2-YFP reveals somato-dendritic staining and colocalization with the presynaptic marker synaptobrevin-2 at synaptic sites. (Left) Hippocampal neurons were stained with an anti-synaptobrevin-2 antibody and visualized with an Alexa 546-coupled secondary antibody. (Middle) Fluorescence patterns of neurons from low-density hippocampal cultures infected with RGS2-YFP reveal a punctuate staining. A punctuate staining similar to that seen with RGS2-YFP was observed. (Right) Overlay of the left and middle picture demonstrates that RGS2-YFP is partially colocalized with the presynaptic marker synaptobrevin-2, as indicated in the yellow staining. Scale bar, 25 μm.

(C–E) Comparison of the paired-pulse ratio (PPR) from autaptic cultures of rat (D), mice, and *RGS2*$^{-/-}$ mice (E) in the absence and presence of exogenously expressed RGS2. Single neuron autapses were voltage-clamped at a holding potential of –60 mV. EPSCs were evoked by pairs of 2 ms depolarizing pulses to 10 mV (50 ms interpulse interval [20 Hz]) every 2 s. Representative sample traces of the summary data in (D) and (E) are shown in panel (C). PPR was calculated as the ratio of the second peak EPSC amplitude to the first one. (D) Exogenously expressed RGS2 significantly reduced the 20 Hz PPR (depression) compared with wild-type controls (**$p < 0.005$). (E) *RGS2*$^{-/-}$ cultures show significantly increased PPR (facilitation) compared with wild-type controls (**$p < 0.005$), and PPR is reduced in *RGS2*$^{-/-}$ and wild-type neurons when RGS2 is exogenously expressed (*$p < 0.05$). Error bars = SEM.

in situ hybridization and found that RGS2 mRNA is detected in hippocampal neurons from wild-type, but not *RGS2*$^{-/-}$, mice (Figure 1A). Exogenous expression of RGS2 tagged with YFP at its N and/or C termini revealed a punctate staining pattern (Figure 1B). These puncta are partially colocalized with the synaptic marker synaptobrevin-2 (Figure 1B), suggesting that RGS2 is transported to synaptic sites.

RGS2 Regulates Short-Term Synaptic Plasticity

To determine if RGS2 is able to modulate synaptic transmission, we characterized short-term synaptic plasticity of autaptic synapses, which hippocampal neurons make onto themselves when cultured alone on microislands. Synaptic transmitter release via two depolarizing pulses separated by 50 ms (20 Hz stimulation) and the ratio between the first and the second elicited excitatory postsynaptic current (EPSC) were compared (paired-pulse ratio [PPR]). To investigate the possibility that RGS2 may function during synaptic transmitter release, our initial experiments were performed on rat hippocampal neurons, while later studies were performed on mouse cultures. Exogenous expression of RGS2 in wild-type autaptic hippocampal cultures from rat as well as from mice reduced the PPR and induced paired-pulse depression (PPD) (Figures 1C–1E). In contrast, recordings from autaptic hippocampal neurons from *RGS2*$^{-/-}$ mice revealed paired-pulse facilitation (PPF) and thus an increase in the PPR (Figures 1C and 1E). Furthermore, the PPF was depressed by exogenous expression of RGS2 to PPRs found in the wild-type cultures (Figure 1E). These results suggest that RGS2 regulates

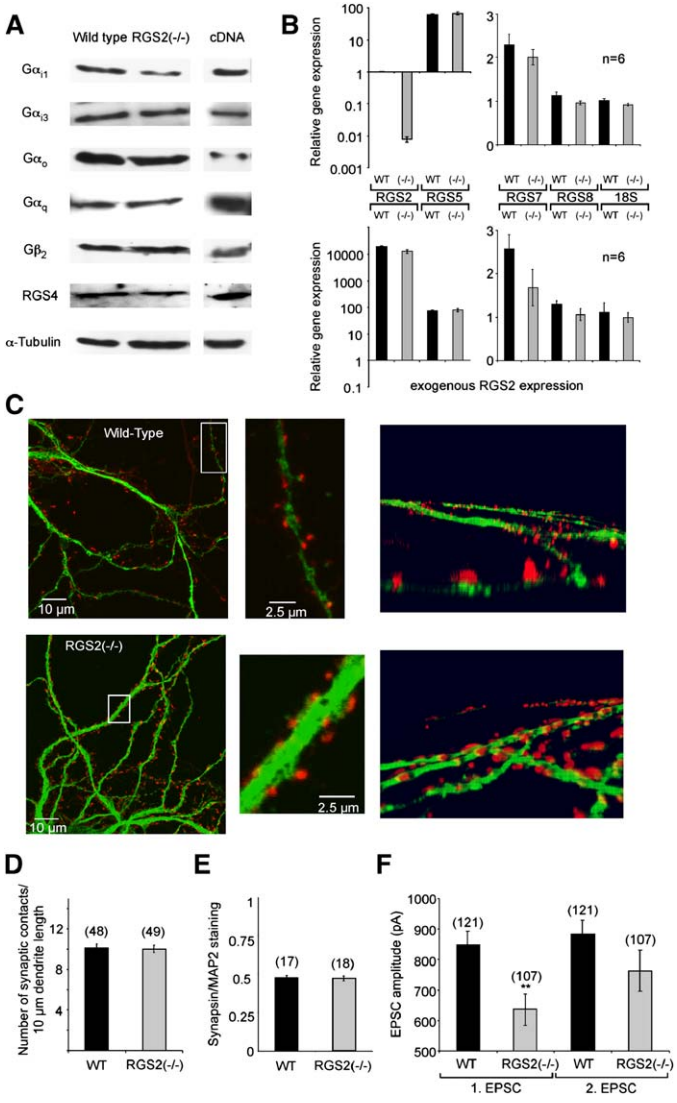

Figure 2. Cultured Hippocampal Neurons from *RGS2*$^{-/-}$ and Wild-Type Mice Have Comparable G Protein Expression and Make Comparable Amounts of Synaptic Contacts

(A) Western blot from 14-day-old wild-type (left) and *RGS2*$^{-/-}$ (middle) cultured hippocampal neurons. The expression of the following endogenous proteins was evaluated with antibodies: $G\alpha_{i1}$, $G\alpha_{i3}$, $G\alpha_{o}$, $G\alpha_{q/11}$, $G\beta_{2}$, and RGS4. Loading control was α-tubulin. As a positive control for the antibody, we transfected HEK293 cells with cDNAs for the indicated proteins (right).

(B) Real time quantitative PCR reveals that neither the absence nor the overexpression of RGS2 (lower panel) changes the relative gene expression of RGS5, 7, and 8. Data are represented relative to the expression of RGS2 in the wild-type neurons. The experiments were performed with three independent neuronal cultures in duplicates (n = 6). A 1:100 dilution of sample was used for 18S as an internal control.

(C) Examples of low-density hippocampal neurons (14 days in culture) from wild-type (upper) and *RGS2*$^{-/-}$ (lower) mice stained with MAP2-antibody (green) and synapsin I-antibody (red). (Middle) Magnification of the indicated region within the neuron (left) and (right). Three-dimensional reconstruction of dendritic arbors from 0.36 µm z-stacks reveal synaptic contacts between the postsynaptic MAP2-labeled neuron and the presynaptic site labeled by synapsin I.

(D and E) The number of synaptic contacts (D) (i.e., the number of synapsin I punctuates per 10 µm MAP2-stained dendrite) and the synapsin I/MAP2 staining ratio (E) (i.e., pixel area stained by synapsin I/MAP2) is comparable between neurons from wild-type and *RGS2*$^{-/-}$ mice.

(F) Comparison of the EPSC amplitudes between autaptic hippocampal neurons from wild-type and *RGS2*$^{-/-}$ mice from the first and second EPSC elicited by two 2 ms long test pulses to +10 mV separated by 50 ms. The EPSCs elicited by the first pulse are significantly different, while the second EPSCs of wild-type and *RGS2*$^{-/-}$ are not, indicating that functional synaptic contacts are sufficiently and comparably formed in both cultures.

Error bars = SEM.

short-term synaptic plasticity, leading to PPF when absent or at low concentrations (Figure 1E), and leading to PPD when available at high concentrations in hippocampal neurons (Figure 1D). To determine if the decrease in PPR is due to changes in expression of various molecules involved in RGS signaling, we compared expression levels of several G proteins and RGS proteins in wild-type and *RGS2*$^{-/-}$ neurons. No significant differences in protein levels of $G\alpha_{i1}$, $G\alpha_{i3}$, $G\alpha_{o}$, $G\alpha_{q/11}$, $G\beta_{2}$, and RGS4 were observed by Western blot analysis in wild-type neurons versus *RGS2*$^{-/-}$ neurons (Figure 2A). In addition, we compared the relative mRNA expression levels of RGS5, 7, and 8 between wild-type and *RGS2*$^{-/-}$ cultures and also observed no significant changes (Figure 2B). Increases in PPR may also reflect changes in neuronal circuit formation due to a reduced number of spines and synaptic contacts formed, as originally suggested for CA1 hippocampal neurons from *RGS2*$^{-/-}$ mice (Oliveira-Dos-Santos et al., 2000). We did not detect a reduction in the number of synapses formed in *RGS2*$^{-/-}$ neurons when they were compared with wild-type neurons (Figures 2C–2E). This is well-supported by the comparison of the mean EPSC amplitudes. While the EPSC amplitudes are significantly different between the *RGS2*$^{-/-}$ and wild-type neurons for the first EPSC during a 20 Hz stimulation, comparison of the EPSC amplitudes elicited by the second pulse during the 20 Hz stimulation revealed no differences, since the *RGS2*$^{-/-}$ neurons have a larger facilitation than wild-type neurons (Figure 2F).

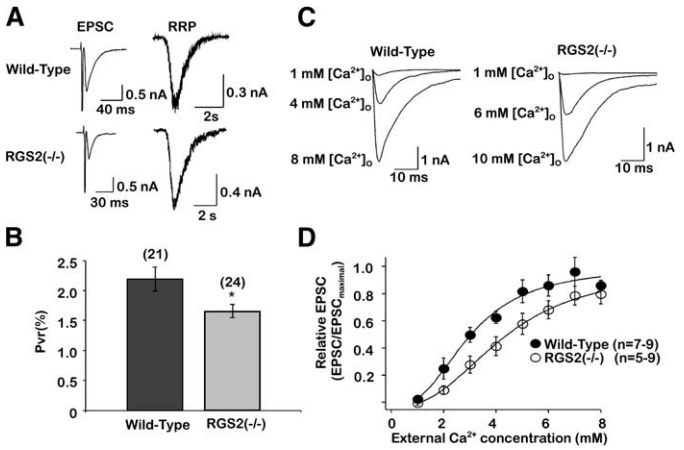

Figure 3. RGS2 Regulates the Probability of Synaptic Vesicle Release and Ca^{2+} Dependence of Transmitter Release

(A) (Left) Examples of EPSCs evoked by 2 ms depolarizing pulses from −60 mV to 10 mV are shown for wild-type neurons (upper) and *RGS2*$^{-/-}$ neurons (lower). (Right) Examples of the hypertonically mediated release of quanta from the same neuron shown on the left upon application of 500 mM sucrose for 4 s.

(B) Probability of synaptic vesicle release was evaluated by calculating the ratio of release evoked by the action potential to that evoked by hypertonic sucrose. In autaptic neurons from *RGS2*$^{-/-}$ mice, the vesicular release probability is significantly reduced compared with wild-type controls (*$p < 0.05$). Error bars = SEM.

(C and D) Varying external Ca^{2+} and Mg^{2+} concentrations from 1 to 8–10 mM and 8–10 to 1 mM, respectively, were applied using an amplifier-controlled perfusion system. (C) Example EPSC traces of wild-type (with extracellular $[Ca^{2+}]_o$ 1 mM, 4 mM, and 8 mM) and *RGS2*$^{-/-}$ neurons (with extracellular $[Ca^{2+}]_o$ 1 mM, 6 mM, and 10 mM). (D) EPSC amplitudes were normalized to the maximal response determined by the free dose response fit for the single experiment. In the absence of RGS2, the midpoint of the curve is shifted to the right, indicating that *RGS2*$^{-/-}$ autapses need higher external Ca^{2+} concentrations to obtain the same synaptic response as the wild-type ones. Error bars = SEM.

The Probability of Synaptic Vesicle Release Is Reduced in *RGS2*$^{-/-}$ Mice Due to a Shift in the Ca^{2+} Dependence of Transmitter Release

To gain a deeper understanding of the precise action of RGS2 on synaptic transmitter release, we analyzed several parameters of synaptic transmission in more detail. A change in the PPR may be caused by an alteration in the vesicle release probability (Thomson, 2000). A low release probability may underlie PPF, while a high release probability may cause PPD. We therefore first compared the probability of synaptic vesicle release between RGS2 knockout and wild-type neurons, which can be examined by comparing the size of the readily releasable vesicle pool (RRP) to the number of vesicles released by a single action potential. The RRP is defined as the number of vesicles released during application of a hypertonic solution (Rosenmund and Stevens, 1996). We found that the vesicle release probability is reduced from the wild-type value of 2.2% to 1.7% in *RGS2*$^{-/-}$ mice when the RRP was compared to the EPSC in each experiment (Figures 3A and 3B), while no differences in the mean RRP size nor the mean EPSC size could be detected due to the small number of neurons analyzed (wild-type: EPSC, 15.4 ± 2.38 [pC], n = 21; RRP, 763 ± 127 [pC], n = 21; *RGS2*$^{-/-}$: EPSC, 14.1 ± 2.18 [pC], n = 24; RRP, 873 ± 108 [pC], n = 24).

This reduction in the probability of release could be caused by a decrease in the amount of available vesicles, an alteration in the recruitment and recycling of the vesicles, a change in the coupling of the vesicles to the release machinery, or a reduction in Ca^{2+} influx through presynaptic Ca^{2+} channels. We first analyzed if the vesicle recycling process within the synaptic terminal was altered. It has previously been observed that $GABA_B$ receptors in the calyx of Held reduce the refilling of synaptic vesicles via cAMP-dependent signaling (Sakaba and Neher, 2003) and that RGS2 negatively regulates several forms of adenylyl cylcase, which could lead to a change in the presynaptic cAMP levels (Kehrl and Sinnarajah, 2002). We therefore depleted the vesicles from the synapses using 30 depolarizing stimuli at a frequency of 20 Hz and analyzed how long it took for the synapse to recover the EPSC amplitude to the level measured before vesicle depletion (Figure 4A). Neither the time constant of EPSC depletion (Figure 4A) or recovery (Figure 4B) nor the amount of recovery of the EPSC (Figure 4B) or the size of the RRP (Figures 4C and 4D) was altered when RGS2 was absent. This suggests that vesicle recycling or priming was not altered in the *RGS2*$^{-/-}$ mice. To exclude postsynaptic and structural/morphological changes of the synapse caused by the absence of RGS2, we also analyzed the miniature EPSCs (mEPSCs) (Figure 4E). mEPSC amplitude (Figure 4F) and mEPSC frequency (Figures 4G and 4H) were not altered in *RGS2*$^{-/-}$ neurons in comparison to wild-type neurons, suggesting that RGS2 does not alter vesicle size or the postsynaptic response to transmitter release.

Differences in PPF and PPD can be caused by changes in the Ca^{2+} entry during repetitive stimulations, resulting in an alteration of the number of transmitter quanta (vesicles) released (Fisher et al., 1997; Zucker, 1999). Therefore, we analyzed the Ca^{2+} dependence of the transmitter release by increasing the external Ca^{2+} concentration between 1 to 10 mM Ca^{2+} and measured the change in EPSC size during 0.2 Hz depolarizing pulses. In the absence of RGS2 protein, the midpoint of the Ca^{2+} dependence of transmitter release curve was shifted to a higher Ca^{2+} concentration (Figures 3C and 3D). This suggests alterations in the Ca^{2+} influx through voltage-dependent Ca^{2+} channels, an alteration in the coupling between presynaptic Ca^{2+} channels and the release machinery, and/or coupling of Ca^{2+} to the vesicle release.

RGS2 Acts on Synaptic Transmission via Modulating $G_{i/o}$, but Not G_q, Pathways

RGS2 accelerates and/or inhibits $G_{i/o}$ pathways and inhibits G_q-coupled receptor pathways in cells (Kehrl and Sinnarajah, 2002). $G_{i/o}$, as well as downstream

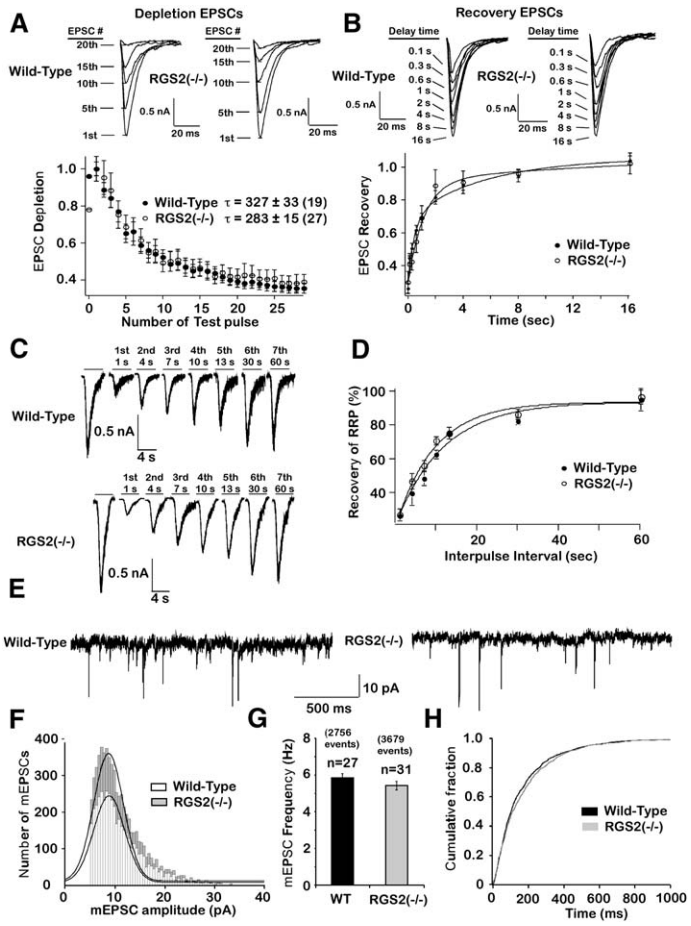

Figure 4. Synaptic Vesicle Recycling and Spontaneous Release Properties Are Not Altered in Hippocampal Neurons from *RGS2*$^{-/-}$ Mice

To evaluate whether RGS2 affects synaptic vesicle recycling, two approaches were applied. (A and B) The amount and time course of depletion of the RRP as well as the recovery of the RRP following activity is not different between *RGS2*$^{-/-}$ cultures and wild-type controls. The depletion was determined by measuring the recovery of the EPSC amplitude at varying time points following depletion induced by 30 2 ms long voltage pulses to 10 mV at 20 Hz. Example traces are shown on top. In (A) (lower), the EPSCs were normalized to the largest EPSC during the 20 Hz stimuli train. In (B) (lower), the recovered EPSCs were normalized to the first EPSC in the 20 Hz stimuli train.

(C and D) The refilling of the RRP was also measured by applying paired pulses of hypertonic solution (500 mM sucrose, each for 4 s) with varying interpulse intervals (1 s, 4 s, 7 s, 10 s, 13 s, 30 s, and 60 s). Example traces are shown in (C). The second response was normalized to the first response, and the quantified data from wild-type and knockout cultures are shown in (D). Again, there was no significant difference between the recovery rates of neurons from wild-type and *RGS2*$^{-/-}$ mice.

(E) Examples of mEPSCs recorded in the presence of 200 nM TTX from wild-type and *RGS2*$^{-/-}$ autaptic hippocampal cultures. The analysis indicated that the amplitude distribution (F) and the frequency (shown as the mean frequency [G] and the interevent interval cumulative fraction [H]) of the spontaneous vesicle release were not significantly altered in the absence of RGS2. This suggests that postsynaptic properties did not change in neuronal cultures from *RGS2*$^{-/-}$ mice. The mean values for the amplitude distribution were: wild-type 11.5 ± 0.1 pA (4510 events, n = 32), *RGS2*$^{-/-}$ 11.4 ± 0.1 pA (6441 events, n = 37). Statistical significance of the interevent interval cumulative fraction plot and the mEPSC amplitude distribution was evaluated with a Kolmogorov-Smirnov 2 sample test ($p > 0.1$). Error bars = SEM.

effectors of the G_q pathways, modulates synaptic transmission. For example, classical presynaptic inhibition is caused by the inhibition of presynaptic Ca^{2+} channels via $G_{i/o}$-pertussis toxin (PTX) sensitive GPCR activation (Stevens, 2004). Downstream components of the G_q pathway, such as diacylglycerol (DAG), increase vesicle priming (Brose et al., 2000), and PKC has been suggested to regulate the size and the refilling rate of the vesicle pool (Morgan et al., 2005). Therefore, alterations in the G_q as well as $G_{i/o}$ pathway in the *RGS2*$^{-/-}$ neurons might underlie the observed changes in PPR. In order to investigate whether the increased PPF in *RGS2*$^{-/-}$ neurons is mediated by $G_{i/o}$ or G_q-coupled pathways, we analyzed transmission in the presence of PTX, which blocks the $G_{i/o}$ pathway, and YM-254890, a specific blocker of the $G_{q/11}$ pathway (Takasaki et al., 2004). We found that incubation of the autaptic neurons with PTX 24 hr prior to the experiments abolished PPF and reduced the PPR of *RGS2*$^{-/-}$ neurons from 1.16 to 0.98, i.e., to levels observed in the wild-type neurons (1.03 ± 0.02 [n = 25], Figure 5). In wild-type neurons PTX did not alter the PPR (Figure 5B). In contrast, blocking the G_q pathway by application of 10 ng/ml YM-254890 did not change PPF in neurons from knockout or wild-type mice (Figures 5A and 5B). To demonstrate that YM-254890 can effectively inhibit G_q pathways at 10 ng/ml, we monitored the G_q-induced PIP_2 hydrolysis with the described PIP_2 sensor PH-EGFP in HEK293 cells (Stauffer et al., 1998). HEK293 cells were transfected with mAChR-M1 receptor and PH-EGFP in a 5:1 molar ratio to guarantee that cells containing the PIP_2 sensor also contain the G_q-coupled receptor mAChR-M1. As shown in Figures 5C and 5D, YM-254890 blocks mAChR-M1-mediated PIP_2 hydrolysis at the plasma membrane. These results taken together suggest that the $G_{i/o}$, but not the G_q, pathway is involved in the increased PPF observed in *RGS2*$^{-/-}$ neurons.

To obtain further evidence that RGS2 mediates its effect via the $G_{i/o}$, but not the G_q, pathway, we analyzed the effect of the RGS2 mutant (N149A) on the $G_{i/o}$ and G_q pathway in *Xenopus* oocytes and on synaptic transmission in neurons. The corresponding amino acid in RGS4 (N128A), which belongs to the same RGS subfamily, has been shown to determine RGS affinity toward the G protein α subunits (Posner et al., 1999). Since RGS2 has a low potency as a GAP in the $G_{i/o}$ pathway, but a high potency as an inhibitor of the G_q pathway (Heximer et al., 1997, 1999), we introduced the point

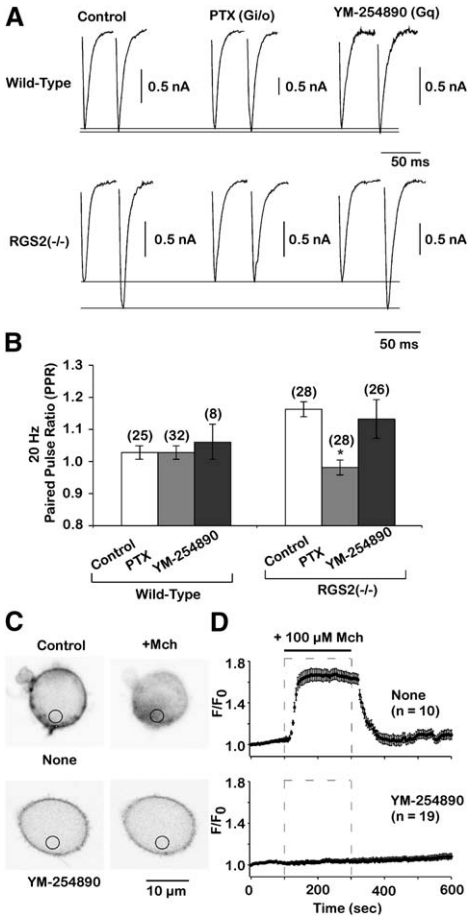

Figure 5. RGS2 Regulates Synaptic Plasticity through PTX-Sensitive Pathways

Single neuron autapses were voltage-clamped at a holding potential of –60 mV. EPSCs were evoked by pairs of 2 ms depolarizing pulses (10 mV) at 50 ms interpulse intervals (20 Hz) every 2 s. (A) Example traces of wild-type and *RGS2*$^{-/-}$ neurons in the presence and absence (left) of PTX (middle) and YM-254890 (right) elicited by a two-pulse 20 Hz stimulation. (B) PTX ($G_{i/o}$ blocker) pretreatment (100 ng/mL, 24 hr) abolished the increased 20 Hz PPR in *RGS2*$^{-/-}$ autapses (**$p < 0.005$), while YM-254890 (G_q blocker) pretreatment (10 ng/mL, 18 hr) had no significant effect. (C and D) Monitoring of intracellular G_q pathways activation by PH-EGFP. (C) Confocal images of HEK293 cells transfected with mAChR-M1 and PH-EGFP before (left) and after (right) application of 100 μM Mch. Images are shown as negative contrast images. Black circles show the cytoplasmic area which was used for comparing the fluorescence intensity. (D) Time course of fluorescence ratio changes (F/F_0) within the cytoplasm during 100 μM Mch application in the presence (lower) and absence (upper) of YM-254890 (10 min and 18 hr pretreatment 10 ng/mL). Error bars = SEM.

mutation N149A into RGS2 under the assumption that the reduced affinity for both pathways would eliminate the effect of RGS2 on the $G_{i/o}$ pathway, but would still be able to block the G_q pathway. To characterize the effect of the mutant RGS2 on the two signaling pathways, we made use of the *Xenopus* oocyte expression system. We and others have demonstrated that RGS2 accelerates the deactivation kinetics of the G protein inward-rectifying potassium (GIRK) channel when the channels were activated by the M_2 muscarinic acetycholine receptor (mAChR-M_2), a $G_{i/o}$-coupled receptor (Doupnik et al., 1997; Herlitze et al., 1999; Mark et al., 2000a). In addition, it was shown that activating the G_q-coupled pathways in *Xenopus* oocytes via GPCRs activates an endogenous Ca^{2+}-activated Cl^- current. The activation of this Cl^- current is blocked by RGS2 and other RGS proteins, and it has been suggested that the RGS effect is due to the inhibitory effect of the RGS on the G_q pathway (Mark et al., 2000a; Saugstad et al., 1996). To evaluate if the RGS2 mutant was still capable of inhibiting the G_q pathway, we coexpressed RGS2 wild-type or RGS2(N149A) together with GIRK1/4 channels and P_2Y_2 receptors. P_2Y_2 receptors, when expressed in *Xenopus* oocytes, activate both the $G_{i/o}$ and G_q pathway (Mosbacher et al., 1998). Activation of the $G_{i/o}$ pathway leads to GIRK channel activation, while stimulation of the G_q pathway activates the endogenous Ca^{2+}-activated Cl^- channels. This current can be measured as an outward current (see arrow in Figure 6A, second trace). Since very little outward K^+ current is detected due to the inward-rectifying properties of the GIRK channel, most of the outward current is mediated by the Cl^- channel. Coexpression of RGS2 (1:2 dilution) or RGS2(N149A) (1:2 dilution) completely suppressed the Ca^{2+}-activated outward current, suggesting that both the wild-type and the RGS2 mutant inhibit the G_q pathway (Figures 6A and 6B). Even upon further dilution, the RGS2(N149A) mutant (1:20) was still able to reduce the G_q-activated Cl^- current significantly, but not completely (Figure 6B). The same effects were observed in our previous study when RGS2 was diluted to 1:40 (see Mark et al., 2000a). We next analyzed if the RGS2 mutant is able to accelerate the deactivation kinetics of GIRK channels once they are activated via the $G_{i/o}$ pathway. We coexpressed the RGS2 proteins together with GIRK1/4 subunits and mAChR-M_2. Activation of mAChR-M_2 via application of 10 μM ACh leads to an increase in GIRK current. Once ACh is washed out the GIRK channel deactivates. The deactivation time depends on the termination of the G protein cycle and is accelerated by RGS proteins including RGS2 (Herlitze et al., 1999; Mark et al., 2000a). As shown in Figures 6C and 6D, the GIRK channel deactivation is faster in the presence of RGS2 but is slowed in the presence of RGS2(N149A). The slowing of the GIRK channel deactivation can be explained by a dominant-negative effect of RGS2(N149A) on the $G_{i/o}$ pathway, since RGS2(N149A) may compete with the endogenous RGS proteins for binding to the $G\alpha_{i/o}$ proteins in *Xenopus* oocytes.

The experiments described above suggest that RGS2(N149A) is still capable of blocking the G_q pathway but has lost its GAP activity on the $G_{i/o}$ pathway, where it now acts as a dominant-negative mutant. Thus, if RGS2 affects short-term synaptic plasticity via the $G_{i/o}$ pathway, we should not be able to depress PPF with this mutant in *RGS2*$^{-/-}$ neurons, but we should be able to induce PPF in the wild-type neurons due to the dominant-negative effect of the mutant. In contrast, if RGS2 affects short-term plasticity via block of the G_q pathway, we should be able to reduce PPF in the knockout neurons, but should see no effect on the wild-type neurons. Exogenous expression of RGS2(N149A) in neurons from *RGS2*$^{-/-}$ mice revealed no effect on PPF, but PPF was increased in wild-type neurons, providing additional evidence that the RGS2 mutant acts on the $G_{i/o}$ pathway

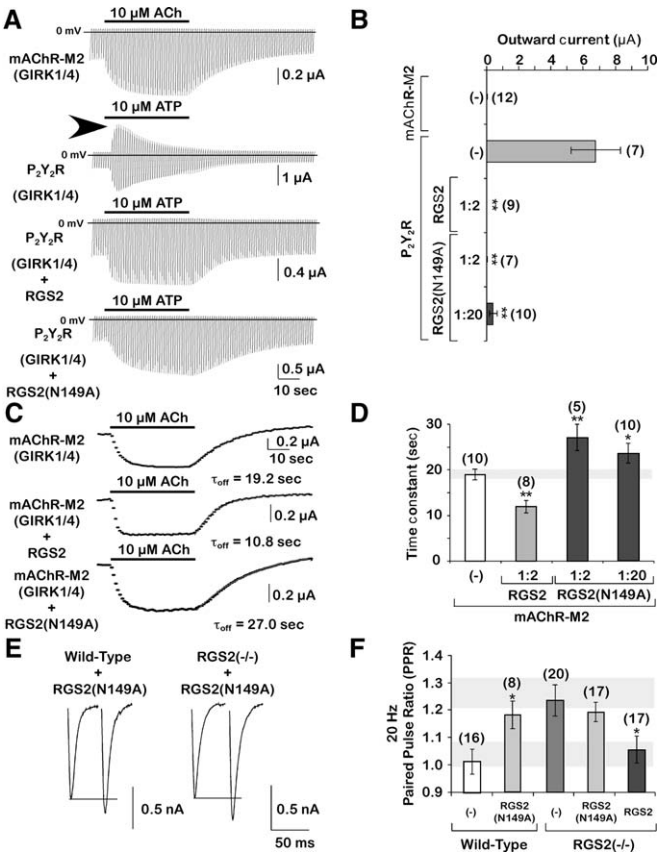

Figure 6. The RGS2 Mutant N149A, which Is Able to Affect the G_q Pathway, But Not the $G_{i/o}$ Pathway, Is Unable to Rescue the Increased PPR in *RGS2*$^{-/-}$ Autapses But Acts as a Dominant-Negative Mutant in Wild-Type Neurons

(A and B) Both RGS2 and RGS2(N149A) inhibit the G_q pathway. (A) Example voltage ramp traces of GIRK1/4 currents elicited from *Xenopus* oocytes coexpressing mAChR-M_2, P_2Y_2-R, P_2Y_2-R and RGS2, and P_2Y_2-R and RGS2(N149A) by application of 10 μM ACh to activate mAChR or 10 μM ATP to activate P_2Y_2-R. Note that the P_2Y_2-R activates not only the $G_{i/o}$ (as mAChR-R does) but also the G_q pathway. This becomes evident in the large Ca^{2+}-activated Cl^- current (arrow, outward current). This outward current is absent when RGS2 or RGS2(N149A) are coexpressed with the P_2Y_2-R, since the G_q pathway is blocked by the RGS2 proteins. (B) In the presence of RGS2 or RGS2(N149A) mutant, the P_2Y_2-R-mediated outward current is drastically reduced or absent, suggesting that the G_q pathway is inhibited. Values from outward currents are the largest outward current detected after application of ATP and were measured at +40 mV.

(C and D) RGS2, but not RGS2(N149A), is able to accelerate the $G_{i/o}$ pathway. (C) Example traces measured at −60 mV of GIRK1/4 currents recorded from *Xenopus* oocytes by activation of mAChR-M_2 coexpressed with or without RGS2 or RGS2(N149A). GIRK deactivation time is accelerated in the presence of RGS2 and slowed in the presence of RGS2(N149A), indicating that RGS2 but not RGS2(N149A) accelerates the $G_{i/o}$ pathway. (D) Comparison of deactivation time constants, derived from a single exponential fit of the deactivation curve as shown in (C).

(E and F) Exogenous expression of RGS2(N149A) in *RGS2*$^{-/-}$ autaptic cultures did not rescue PPR, but increased the PPR in wild-type neurons, suggesting that RGS2(N149A) can act as a dominant-negative mutant on the $G_{i/o}$ pathway. (E) Example EPSC traces of RGS2(N149A) exogenously expressed in wild-type and *RGS2*$^{-/-}$ neurons elicited by a two-pulse 20 Hz stimulation. (F) Comparison between the PPRs of wild-type and *RGS2*$^{-/-}$ neurons exogenously expressing RGS2 or RGS2(N149A).

Error bars = SEM.

in a dominant-negative way (Figures 6E and 6F) and that RGS2 influences synaptic transmitter release at the presynaptic terminal.

Non-L-type Ca^{2+} Channels Exhibit Increased G Protein Modulation in Hippocampal Neurons from *RGS2*$^{-/-}$ Mice

The results suggest that the basal activity of G proteins of the $G_{i/o}$ family is higher in *RGS2*$^{-/-}$ mice since PTX inhibits the activation of this G protein family via ADP-ribosylation of the G protein α subunit. The increased activity of the G protein is probably due to the reduced level of RGS proteins, which in turn prolong the activation of the $G_{i/o}$ protein cycle. This predicts a higher concentration of active G protein subunits (i.e., $G\alpha_{i/o}$ or $G\beta\gamma$ subunits) within the cell and the presynaptic terminal. We have shown that presynaptic Ca^{2+} channels are modulated directly via G protein βγ subunits, leading to the inhibition of the channels (Herlitze et al., 1996; Ikeda, 1996). In addition, $G\beta\gamma$ subunits mediate presynaptic Ca^{2+} channel inhibition at the calyx of Held (Kajikawa et al., 2001). The voltage-dependent inhibition of the Ca^{2+} channels can be released by high positive prepulses, a process defined as prepulse facilitation (Elmslie et al., 1990). The amount of prepulse facilitation provides an indication of the degree to which the channels are modulated by G protein βγ subunits (Zamponi and Snutch, 1998). We therefore tested if the prepulse facilitation of somatic non-L-type channels (mainly P/Q- and N-type channels) would be increased in the *RGS2*$^{-/-}$ neurons, suggesting increased levels of active $G_{i/o}$ proteins. In the presence of TTX to block Na^+ channels and DHPs to block L-type channels, somatic Ca^{2+} currents were elicited by two test pulses to the same test potentials. Before the second test pulse, a high positive prepulse was elicited to release G protein modulation (Figure 7B). The peak current ratios of the currents before and after the prepulse were compared to determine the amount of facilitation. Indeed, prepulse facilitation was increased from 1.0 to 1.8 in *RGS2*$^{-/-}$ neurons (Figures 7B and 7C). To further verify this result, we compared the IV relationship of the non-L-type Ca^{2+} currents in the neuronal cultures. As predicted for G protein-modulated channels, the peak amplitude of the Ca^{2+} current was shifted by 4 mV to more depolarized potentials with no change in the reversal potential (Figures 7D and 7F). This most likely reflects the slower opening of the channel and/or a shift in the voltage

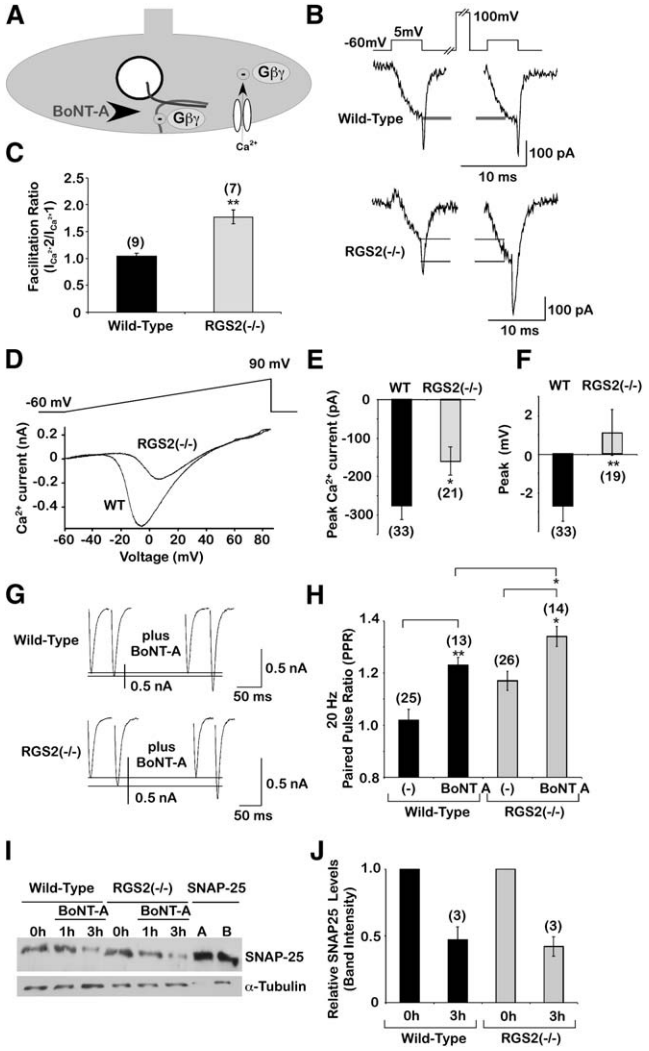

Figure 7. G Protein-Mediated Ca^{2+} Channel Inhibition Is Increased in Hippocampal Neurons from *RGS2*$^{-/-}$ Mice, while BoNT-A Has Similar Effects on the Release Probability and PPR of Neurons from Wild-Type and RGS2 Knockout Mice

(A) A diagram to show that increased Gβγ levels in the presynaptic terminal may reduce transmitter release by inhibition of presynaptic Ca^{2+} channels or by binding to SNAP-25 to interfere with vesicle fusion. BoNT-A partially cleaves SNAP-25, which causes PPF in hippocampal neurons.

(B and C) Ca^{2+} currents were elicited from a holding potential of −60 mV by a 10 ms test pulse to +5 mV. After 2 s, a 10 ms prepulse to +100 mV was applied, and a second 10 ms test pulse to +5 mV was elicited after stepping back for 10 ms to −60 mV. Facilitation ratios were determined by dividing the peak current of test pulse 2 by the peak current of test pulse 1. (B) Examples of traces recorded from wild-type and *RGS2*$^{-/-}$ neurons indicating that, in the absence of RGS2, G protein modulation of the Ca^{2+} channels is increased. (C) A diagram of the quantified Ca^{2+} current facilitation ratios indicates again that in the absence of RGS2, G protein modulation of Ca^{2+} currents is increased (***$p < 0.0005$).

(D) Example current traces (IV curve) of non-L-type currents from wild-type and *RGS2*$^{-/-}$ neurons elicited by a 500 ms voltage ramp from −60 to +90 mV. The comparison of the traces reveals a positive shift in the peak inward current with no change in the reversal potential.

(E) Diagram of the averaged peak currents of currents elicited by the voltage ramp demonstrates that the non-L-type Ca^{2+} currents are reduced in the absence of RGS2 (*$p < 0.04$).

(F) Diagram of the voltage at which the peak current appears during the voltage ramp. The diagram shows that the peak current is shifted to more positive potentials in *RGS2*$^{-/-}$ neurons (**$p < 0.007$).

(G and H) Application of BoNT-A increases PPR of both wild-type and *RGS2*$^{-/-}$ neurons, suggesting that the main action of Gβγ in reducing transmitter release is via inhibition of presynaptic Ca^{2+} channels. (G) Examples of EPSC traces of wild-type and *RGS2*$^{-/-}$ neurons in the presence and absence of BoNT-A elicited by a two-pulse 20 Hz stimulation. (H) Comparison of the PPR from autaptic cultures of wild-type mice and *RGS2*$^{-/-}$ mice in the presence or absence of BoNT-A. Single-neuron autapses were voltage-clamped at a holding potential of –60 mV. EPSCs were evoked by pairs of 2 ms depolarizing pulses (10 mV) (50 ms interpulse interval [20 Hz]) every 2 s. PPR was calculated as the ratio of the second peak EPSC amplitude to the first one. In the presence of BoNT-A in *RGS2*$^{-/-}$ as well as wild-type cultures, PPR (facilitation) is significantly increased (*$p < 0.05$; **$p < 0.01$).

(I) Western blot analysis of endogenous SNAP-25 from wild-type and *RGS2*$^{-/-}$ hippocampal cultures before and after BoNT-A (0.2 nM) treatment for 1 and 3 hr. α-tubulin was used as a loading control. As a positive control for the antibody, we transfected HEK293 cells with cDNAs for SNAP-25 A and B.

(J) Quantification of the relative amount of SNAP-25 after 3 hr of BoNT-A treatment. After 3 hr of BoNT-A treatment, SNAP-25 protein is reduced by 50%–60% when compared with control protein levels in wild-type and *RGS2*$^{-/-}$ neurons.

Error bars = SEM.

dependence of activation to more depolarized potentials. Both effects have been attributed to the modulation of voltage-gated Ca^{2+} channels by G protein βγ subunits (Herlitze et al., 1996; Ikeda, 1996). In addition, the average amplitudes of the peak Ca^{2+} currents were reduced in the *RGS2*$^{-/-}$ neurons (Figure 6E), thereby supporting the increased inhibition of the Ca^{2+} channels by Gβγ subunits.

The results suggest that RGS2 regulates Ca^{2+} influx through voltage-gated Ca^{2+} channels into presynaptic terminals by reducing the basal activity of the $G_{i/o}$ protein family.

Botulinum Toxin A Decreases the Release Probability and Induces PPF of both RGS2 Knockout and Wild-Type Hippocampal Neurons

It has been shown that Gβγ inhibits synaptic transmission in the lamprey neurons downstream of Ca^{2+} entry (Blackmer et al., 2001) (Figure 7A). Increased Gβγ protein levels may therefore, in addition to modulating Ca^{2+} influx, also act directly at the presynaptic vesicle release machinery. More detailed studies show that Gβγ most likely interferes with vesicle fusion by binding to SNAP-25 (Blackmer et al., 2005), thereby causing a reduction in transmitter release. In those experiments the

specific cleavage of SNAP-25 by BoNT-A prevented additional transmitter- and Gβγ-mediated synaptic inhibition. Therefore, in our system, if Gβγ is acting on SNAP-25 to prevent transmitter release, partial cleavage of SNAP-25 in neurons from RGS2 knockout mice should not significantly increase PPF as would be expected in the wild-type mice (Young, 2005). We therefore incubated the wild-type and *RGS2*$^{-/-}$ autaptic hippocampal neurons with BoNT-A for 3 hr prior to the experiment, which leads to a 50%–60% reduction in the SNAP-25 protein levels (Figures 7I and 7J), and compared the PPR of these with those of neurons incubated without BoNT-A. As expected, application of BoNT-A increased the PPR from 1.02 to 1.23 in wild-type mice (Figures 7G and 7H). Interestingly, an increase in PPR from 1.17 to 1.34 was also observed in the *RGS2*$^{-/-}$ neurons (Figures 7G and 7H). The PPR in *RGS2*$^{-/-}$ neurons treated with BoNT-A was significantly larger than the PPR in wild-type neurons, revealing that cleavage of SNAP-25 is affecting synaptic transmission of *RGS2*$^{-/-}$ and wild-type neurons in a similar fashion. This suggests that inhibition of synaptic transmission by Gβγ is mediated via inhibition of presynaptic Ca^{2+} channels and not mediated via binding to the SNARE complex. However, since it is not possible to completely cleave SNAP-25 without blocking transmitter release, the experiments have to be interpreted carefully in respect to variations in SNAP-25 cleavage and to the possibility that the remaining SNAP-25 is the target of Gβγ action.

Discussion

We demonstrate here that one of the small RGS family members, RGS2, regulates synaptic strength. In the presence of RGS2, transmitter release probability is high, while in the absence of RGS2, synaptic transmitter release probability is reduced. Our data help to explain the effects previously observed in RGS2 knockout mice (i.e., reduced synaptic activity [Oliveira-Dos-Santos et al., 2000]), give mechanistic insight into the action of RGS2 on synaptic function, and point to an importance in regulating RGS2 expression during neuronal activity for regulating neuronal circuits and behavior. The physiological consequences and the molecular mechanisms of RGS2 controlling synaptic transmitter release are discussed below.

Physiological Consequences of RGS2 Expression

RGS2 knockout mice reveal increased anxiety and reduced male aggression, which is correlated with a reduction in synaptic transmission in CA1 hippocampal neurons (Oliveira-Dos-Santos et al., 2000). Further studies of the RGS2 knockout mice reveal an important function for RGS2 in blood pressure control (Tang et al., 2003). Genetic dissection of trait loci also suggests that RGS2 plays an important role in anxiety (Yalcin et al., 2004). These studies suggest that RGS2 is involved in regulating neuronal circuits underlying autonomic nervous system regulation and animal behavior. Our study provides an explanation of how RGS2 can modulate the synaptic output in the brain: high expression levels of RGS2 increase synaptic strength, while low expression levels decrease synaptic strength. Since RGS2 is an immediate early gene, which is upregulated very efficiently during activity-dependent processes, at least in certain brain areas (Burchett, 2005; Burchett et al., 1998; Ingi et al., 1998), our results suggest that the level of RGS2 proteins within a certain neuronal population will define their synaptic efficacy via regulating the basal activity of G proteins of the $G_{i/o}$ family.

Mechanistic Insight into the Function of RGS2 in Neurons

Our initial finding, i.e., that PPF is increased in the absence of RGS2, suggested a reduction in the synaptic release probability. A reduction in the release probability can be caused by altering several processes during transmitter release which involve $G_{i/o}$ and/or G_q-coupled receptor pathways. Classical presynaptic inhibition is mediated by GPCRs, which couple to the PTX-sensitive $G_{i/o}$ proteins, where the Gβγ subunits inhibit presynaptic Ca^{2+} channels and reduce Ca^{2+} influx during potential changes at the synaptic terminal (Herlitze et al., 1996; Ikeda, 1996; Kajikawa et al., 2001). We found in the RGS2 knockout mice that non-L-type channels (i.e., mostly the presynaptic channel types N and P/Q) in hippocampal neurons reveal a stronger voltage-dependent G protein inhibition in comparison with wild-type neurons, suggesting that the level of G protein βγ subunits in the *RGS2*$^{-/-}$ neurons is higher. An increased basal activity level of the $G_{i/o}$ pathway in neurons would explain the elevated Gβγ protein levels. This basal activity is normally very low, as has been estimated by the tonic inhibition of Ca^{2+} currents at the presynaptic terminal of the calyx of Held (Cuttle et al., 1998). In fact, increased constitutive activity of GPCRs has been shown to play a role in causing diseases such as cancer, cardiac hypertrophy, and hypertension (Seifert and Wenzel-Seifert, 2002). Our data also correlate well with the recent finding that increased expression of RGS4 in striatal cholinergic interneurons decreases mAChR-M4-mediated Ca^{2+} channel inhibition (Ding et al., 2006).

G protein βγ subunits act on several synaptic effector proteins besides the presynaptic Ca^{2+} channels. It has been shown that Gβγ interacts with several components of the synaptic release machinery (Jarvis and Zamponi, 2001) and that Gβγ can lead to decreased transmitter release downstream of Ca^{2+} entry (Blackmer et al., 2001), most likely via direct binding to the SNARE protein SNAP-25 (Blackmer et al., 2001, 2005; Gerachshenko et al., 2005). This conclusion was drawn based on the fact that BoNT-A, which cleaves SNAP-25, prevented the serotonin-induced, Gβγ-mediated synaptic inhibition. In contrast, BoNT-B, which specifically cleaves synaptobrevin, did not prevent serotonin's effect on transmission. We therefore tested the possibility that the increased concentration of free Gβγ in the presynaptic terminal would occlude effects of BoNT-A, as would be expected if Gβγ inhibits transmitter release via binding to SNAP-25. Since partial cleavage of SNAP-25 further reduced transmitter release in the *RGS2*$^{-/-}$ neurons in comparison with wild-type neurons, our results suggest that the reduction of transmitter release by increased Gβγ levels is mediated primarily by reducing Ca^{2+} influx through presynaptic Ca^{2+} channels. Another possibility for RGS2 function at the presynaptic terminal is that the $G_{i/o}$ pathway may inhibit adenylate cyclase

(for example, via $GABA_B$ receptors [Sakaba and Neher, 2003]), leading to a decrease in cAMP levels. Indeed, RGS2 has been described to inhibit the activity of certain adenylyl cyclase isoforms and thus reduce cAMP levels (Kehrl and Sinnarajah, 2002). Decreased cAMP levels and inhibition of adenylate cyclase in the presynaptic terminal results in attenuation of vesicle recruitment to the RRP, an effect which is mediated by the cAMP-dependent guanosine exchange factor (cAMP-GEF) and not by PKA. PKA by itself seems to play a role in synaptic transmission by increasing or maintaining the vesicle pool size (RRP and slowly releasable pool [SRP]), an effect which is counteracted by the Ca^{2+}/calmodulin-dependent protein phosphatase calcineurin (Nagy et al., 2004). However, we did not observe any alterations in synaptic vesicle cycling, suggesting that RGS2 inhibits synaptic transmitter release by modulating Ca^{2+} entry into the presynaptic terminal.

RGS2 has the capacity to accelerate $G_{i/o}$ and to antagonize G_q pathways (Kehrl and Sinnarajah, 2002), but it has been suggested to have a greater affinity for $G\alpha_q$ than for $G\alpha_{i/o}$ proteins (Heximer et al., 1999). Therefore, recent studies have concentrated on the effects of RGS2 on modulating G_q-coupled pathways in heterologous expression systems and intact tissues, where RGS2, for example, regulates the Ca^{2+} oscillation, adaptation, and excitability of pancreatic acini via regulating intracellular IP_3 levels (Wang et al., 2004). It was therefore surprising to observe that the loss of RGS2 protein and overexpression of RGS2 in neuronal hippocampal cultures seems to act via the $G_{i/o}$ pathway rather than the G_q pathway, at least in the presynaptic terminal. Neither blockers of the G_q pathway nor the point mutation of RGS2, which abolishes its effects on the $G_{i/o}$ pathway while maintaining modulation of the G_q pathway, were effective in rescuing RGS2 deficiencies. On the other hand, PTX was sufficient to block the PPF effect in *RGS2*$^{-/-}$ mice, and the RGS2(N149A) mutant acted as a dominant-negative mutant for RGS2 function by increasing the PPF. These results suggest that the major targets of RGS2 within the presynaptic terminal are GPCRs, which couple to the $G_{i/o}$ pathway. This conclusion is also supported by the fact that vesicle recycling in *RGS2*$^{-/-}$ mice is normal, since several second messengers within the G_q pathway, including DAG and PKC, have been described to modulate synaptic transmitter release at the level of vesicle priming and recycling (Morgan et al., 2005; Nagy et al., 2004; Rhee et al., 2002). Therefore, increased G_q signaling in the absence of RGS2 would have been expected to cause increased PLC activation, increased DAG synthesis, and increased Munc13 activation, resulting in faster vesicle priming and less depression during high-frequency trains. In contrast, inhibition of G_q pathways by RGS2 would have been expected to increase depression. In both cases the time course of vesicle recycling should be altered. This was, however, not the case, pointing again to RGS2 acting primarily on the $G_{i/o}$ pathway, rather than the G_q pathway, during short-term synaptic plasticity.

In summary, we show that RGS2 regulates synaptic output. The importance of this finding lies in the underestimated effects of RGS2 on modulating the $G_{i/o}$ pathway, the important function of RGS2 in regulating the basal activity of the $G_{i/o}$ pathway within a neuron, and in the possibility that upregulation of RGS2 in certain neuronal circuits will most likely modulate synaptic strength.

Experimental Procedures

cDNA Constructs, Viral Production and Infection, and Cell Culture

Mouse RGS2, 4, 5, 8 cDNA (Herlitze et al., 1999; Mark et al., 2000b), mouse RGS7 (Accession number BC051133), G protein $\alpha_{i1,3,o}$ and $G\beta_2$ (Herlitze et al., 1996), mouse $G\alpha_q$ (Accession number M55412, gift from Dr. M. Simon, Pasadena, CA) and SNAP-25A and B (gift from Dr. M. Wilson, Albuquerque, NM) were cloned into mammalian expression vectors (pcDNA variants) for expression in HEK293 cells. RGS2 cDNA was also cloned into the SinRep(nsP2S726)dSP-EGFP virus vector and also cloned for the initial recordings in rat into pSFV. For localization studies the RGS2 was inserted into pEYFP-N1 and pEYFP-C1 (Clontech). The point mutation RGS2(N149A) was introduced into RGS2 using an overlap extension PCR method (Herlitze and Koenen, 1990; Ho et al., 1989). The point mutation was confirmed by DNA sequencing, and the cDNA carrying the mutation was cloned into SinRep(nsP2S726)dSP-EGFP and pBF1 (oocyte expression). PH-EGFP was a gift from Dr. T. Meyer (Stauffer et al., 1998). Sindbis pseudovirions were prepared according to Invitrogen's instructions (Sindbis Expression System) and as published in our recent publication (Li et al., 2005). For RGS2 overexpression and rescue experiments, cultured neurons were infected with 50 μl of sindbis pseudovirions containing the cDNAs of RGS2 or RGS2(N149A) constructs. Recordings were performed up to 24 hr post infection. Microisland and continental cultures of hippocampal neurons were prepared according to a modified version of published procedures from mouse or rat pups (P0-3) (Bekkers and Stevens, 1991; Wittemann et al., 2000).

Immunocytochemistry, Imaging, and Western Blot

Continental hippocampal cultures were prepared as described above and transfected with RGS2-YFP by using the Ca^{2+} phosphate method (Park et al., 2004). 24 hr after transfection, neurons were fixed with 4% paraformaldehyde and permeabilized with 0.2% Triton X-100 in PBS. Anti-GFP (Molecular Probes) and anti-synaptobrevin-2 (SYSY) antibodies were used to label RGS2 and the synaptic marker synaptobrevin-2. Neurons were incubated with the primary antibody overnight at 4°C, washed, then incubated with Alexa 488- and Alexa 568-conjugated secondary antibody (Molecular Probes) for 30 min at room temperature. Cells were embedded in Prolong Gold antifade (Molecular Probes). For the calculation of the number of synapses and synapsin/MAP2 staining ratio, low-density hippocampal cultures were prepared, fixed, and stained as described above. Anti-synapsin I (Invitrogen) and anti-MAP2 (Sigma) antibodies were visualized with Texas red and Alexa 488-conjugated secondary antibodies. Images were acquired with a Zeiss LSM 410 or 510 confocal microscope and analyzed by using VOLOCITY software (Improvision). Western blots from 14-day-old hippocampal neurons from wild-type and *RGS2*$^{-/-}$ mice were performed according to published procedures (Wittemann et al., 2000). Antibodies were from Santa Cruz ($G\alpha_{i1}$, $G\alpha_{i3}$, $G\alpha_o$, $G\alpha_{q/11}$, $G\beta_2$) and RGS4 antibody was a gift from Dr. S. Mumby, Southwestern University, TX. For monitoring the G_q-coupled receptor activation with the PH-EGFP constructs, HEK293 cells were transfected in a 5:1 molar ratio with mAChR-M1 and PH-EGFP. 24 hr after transfection cells were continuously perfused with extracellular recording solution. GFP fluorescence was monitored on the Zeiss LSM 510 inverted confocal microscope at room temperature using a 63× air objective. Pictures were taken every 5 s and analyzed using VOLOCITY software (Improvision). 100 μM Mch (acetyl-B-methylcholine chloride, Sigma) was applied within 2 min and the average fluorescence intensity in a defined cytoplasmic region was normalized to the average intensity before the application of the drug ($F_0 \times (F/F_0)$).

In Situ Hybridization

In situ hybridization was performed as described previously by Schaeren-Wiemers and Gerfin-Moser (1993) and as described in the Supplemental Data.

Real Time Quantitative PCR

Total RNA was subtracted from 14 DIV cultured neurons with RNeasy Mini Kit (Qiagen Inc.) and purified with on-column DNase digestion using RNase-Free DNase Set (Qiagen Inc.). For RT-PCR, 1 μg of RNA was used for reverse transcription with Advantage RT-for-PCR Kit (BD Biosciences) to generate 100 μl cDNA. 3 μl of the final RT product was used for real time PCR for RGS2, 5, 7, 8, and 18S RNA. Real time PCR quantification was performed on iCycler Iq Detection System (Bio-Rad) with CYBR Green assay (Bio-Rad), and DNA fragments of RGS2, 5, 7, 8, and 18S RNA were amplified with primer pairs given in the Supplemental Data. The PCR reactions used a modified 2-step profile with an initial denaturation step for 3 min at 95°C, followed by 40 cycles of 15 s denaturation at 95°C and 25 s polymerase reaction at 57°C. For internal control, 3 μl of 1:100 diluted RT product was used for the 18S reaction with every run so that the 18S cyber threshold (Ct) value was reported in the same range of those of the RGS2 fragments to give more accurate comparison. Relative gene expression data was analyzed with 2-ΔΔCT method (Livak and Schmittgen, 2001).

Electrophysiology and Data Analysis

For EPSC measurements, currents were elicited by a 2 ms long test pulse to 10 mV and recorded and analyzed as published previously (Wittemann et al., 2000). Sucrose solution and various extracellular $[Ca^{2+}]_o$ solutions were applied directly onto the recorded neurons by using a fast-flow perfusion system (ALA Scientific Instruments). The EPSC and RRP charge was calculated by integrating the currents elicited by the single action potential or the sucrose application. The Ca^{2+} response curves were fitted according to the Hill equation: $EPSC = EPSC_{maximal}/(1 + (EC_{50}/[Ca^{2+}]_o)^{Hill\ coefficient})$. The fit values from each curve were used to normalize the dose response curves. The mEPSCs amplitude histograms were plotted with 0.5 pA bins and were fitted with a Gaussian function. mEPSC analysis was performed manually using Mini Analysis Program (Synaptosoft) with an amplitude threshold of 5 pA. 100 ng/ml PTX (Sigma), 10 ng/ml YM-254890 (gift from Dr. Brian Roth) and 0.2 nM BoNT-A (Sigma) were applied 24 hr, 18 hr, and 3 hr, respectively, prior to recordings onto the neuronal cultures. Two microelectrode voltage-clamp recordings were performed as extensively described in our recent paper (Mark et al., 2000a) and as given in the Supplemental Data. Briefly, *Xenopus* oocytes expressing GIRK1/4 and mAChR-M_2 or P_2Y_2-R together with or without RGS2 or RGS2(N149A) (see Supplemental Data for mRNA synthesis, *Xenopus* oocyte preparation, and mRNA injection) were voltage-clamped at 0 mV for 20 ms. Then a 960 ms long voltage ramp from −100 to +50 mV was applied, which then stepped back to 0 mV for 20 ms. This 1 s long protocol was repeated 100 times. Transmitters (10 μM ACh and 10 μM ATP) were typically applied after 10 s for 30 s and then washed out. Time constants for deactivation curves were calculated at −65 mV and were determined with a single exponential fit. The Ca^{2+}-activated Cl^- current (outward current) was measured at +40 mV. Here the largest outward current, which was elicited by 10 μM ATP, was used for analysis. The extracelluar recording solution was a modified Ringer's solution given in the Supplemental Data. Recording solutions for EPSC measurements and non-L-type channel recordings are described (Li et al., 2005) and given in the Supplemental Data.

Statistical significance throughout the experiments was tested with ANOVA by using IGOR software unless otherwise indicated. Standard errors are given as mean ± SEM.

All experiments were approved by the Institutional Animal Research Facility.

Supplemental Data

The Supplemental Data for this article can be found online at http://www.neuron.org/cgi/content/full/51/5/575/DC1/.

Acknowledgments

We thank Drs. E.S. Deneris and L.T. Landmesser for reading the manuscript, Dr. B. Roth for the YM-254890, Dr. S. Mumby for the RGS4 antibody, and Dr. M. Wilson for the SNAP-25 cDNAs. This work was supported by National Institutes of Health Grants NS0447752 and NS42623 to S.H.

Received: February 27, 2006
Revised: June 6, 2006
Accepted: July 14, 2006
Published: September 6, 2006

References

Bekkers, J.M., and Stevens, C.F. (1991). Excitatory and inhibitory autaptic currents in isolated hippocampal neurons maintained in cell culture. Proc. Natl. Acad. Sci. USA *88*, 7834–7838.

Blackmer, T., Larsen, E.C., Takahashi, M., Martin, T.F., Alford, S., and Hamm, H.E. (2001). G protein βγ subunit-mediated presynaptic inhibition: regulation of exocytotic fusion downstream of Ca^{2+} entry. Science *292*, 293–297.

Blackmer, T., Larsen, E.C., Bartleson, C., Kowalchyk, J.A., Yoon, E.J., Preininger, A.M., Alford, S., Hamm, H.E., and Martin, T.F. (2005). G protein βγ directly regulates SNARE protein fusion machinery for secretory granule exocytosis. Nat. Neurosci. *8*, 421–425.

Brose, N., Rosenmund, C., and Rettig, J. (2000). Regulation of transmitter release by Unc-13 and its homologues. Curr. Opin. Neurobiol. *10*, 303–311.

Burchett, S.A. (2005). Psychostimulants, madness, memory… and RGS proteins? Neuromolecular Med. *7*, 101–127.

Burchett, S.A., Volk, M.L., Bannon, M.J., and Granneman, J.G. (1998). Regulators of G protein signaling: rapid changes in mRNA abundance in response to amphetamine. J. Neurochem. *70*, 2216–2219.

Calakos, N., Schoch, S., Sudhof, T.C., and Malenka, R.C. (2004). Multiple roles for the active zone protein RIM1α in late stages of neurotransmitter release. Neuron *42*, 889–896.

Cuttle, M.F., Tsujimoto, T., Forsythe, I.D., and Takahashi, T. (1998). Facilitation of the presynaptic Ca^{2+} current at an auditory synapse in rat brainstem. J. Physiol. *512*, 723–729.

De Vries, L., Zheng, B., Fischer, T., Elenko, E., and Farquhar, M.G. (2000). The regulator of G protein signaling family. Annu. Rev. Pharmacol. Toxicol. *40*, 235–271.

Ding, J., Guzman, J.N., Tkatch, T., Chen, S., Goldberg, J.A., Ebert, P.J., Levitt, P., Wilson, C.J., Hamm, H.E., and Surmeier, D.J. (2006). RGS4-dependent attenuation of M(4) autoreceptor function in striatal cholinergic interneurons following dopamine depletion. Nat. Neurosci. *9*, 832–842.

Doupnik, C.A., Davidson, N., Lester, H.A., and Kofuji, P. (1997). RGS proteins reconstitute the rapid gating kinetics of Gβγ -activated inwardly rectifying K^+ channels. Proc. Natl. Acad. Sci. USA *94*, 10461–10466.

Elmslie, K.S., Zhou, W., and Jones, S.W. (1990). LHRH and GTPγS modify calcium current activation in bullfrog sympathetic neurons. Neuron *5*, 75–80.

Fisher, S.A., Fischer, T.M., and Carew, T.J. (1997). Multiple overlapping processes underlying short-term synaptic enhancement. Trends Neurosci. *20*, 170–177.

Gerachshenko, T., Blackmer, T., Yoon, E.J., Bartleson, C., Hamm, H.E., and Alford, S. (2005). Gβγ acts at the C terminus of SNAP-25 to mediate presynaptic inhibition. Nat. Neurosci. *8*, 597–605.

Hamm, H.E. (1998). The many faces of G protein signaling. J. Biol. Chem. *273*, 669–672.

Herlitze, S., and Koenen, M. (1990). A general and rapid mutagenesis method using polymerase chain reaction. Gene *91*, 143–147.

Herlitze, S., Garcia, D.E., Mackie, K., Hille, B., Scheuer, T., and Catterall, W.A. (1996). Modulation of Ca^{2+} channels by G-protein βγ subunits. Nature *380*, 258–262.

Herlitze, S., Ruppersberg, J.P., and Mark, M.D. (1999). New roles for RGS2, 5 and 8 on the ratio-dependent modulation of recombinant GIRK channels expressed in Xenopus oocytes. J. Physiol. *517*, 341–352.

Heximer, S.P., Watson, N., Linder, M.E., Blumer, K.J., and Hepler, J.R. (1997). RGS2/G0S8 is a selective inhibitor of Gqα function. Proc. Natl. Acad. Sci. USA *94*, 14389–14393.

Heximer, S.P., Srinivasa, S.P., Bernstein, L.S., Bernard, J.L., Linder, M.E., Hepler, J.R., and Blumer, K.J. (1999). G protein selectivity is a determinant of RGS2 function. J. Biol. Chem. *274*, 34253–34259.

Ho, S.N., Hunt, H.D., Horton, R.M., Pullen, J.K., and Pease, L.R. (1989). Site-directed mutagenesis by overlap extension using the polymerase chain reaction. Gene *77*, 51–59.

Ikeda, S.R. (1996). Voltage-dependent modulation of N-type calcium channels by G-protein $\beta\gamma$ subunits. Nature *380*, 255–258.

Ingi, T., Krumins, A.M., Chidiac, P., Brothers, G.M., Chung, S., Snow, B.E., Barnes, C.A., Lanahan, A.A., Siderovski, D.P., Ross, E.M., et al. (1998). Dynamic regulation of RGS2 suggests a novel mechanism in G-protein signaling and neuronal plasticity. J. Neurosci. *18*, 7178–7188.

Jarvis, S.E., and Zamponi, G.W. (2001). Interactions between presynaptic Ca^{2+} channels, cytoplasmic messengers and proteins of the synaptic vesicle release complex. Trends Pharmacol. Sci. *22*, 519–525.

Kajikawa, Y., Saitoh, N., and Takahashi, T. (2001). GTP-binding protein $\beta\gamma$ subunits mediate presynaptic calcium current inhibition by GABA(B) receptor. Proc. Natl. Acad. Sci. USA *98*, 8054–8058.

Kehrl, J.H., and Sinnarajah, S. (2002). RGS2: a multifunctional regulator of G-protein signaling. Int. J. Biochem. Cell Biol. *34*, 432–438.

Li, X., Gutierrez, D., Hanson, M.G., Han, J., Mark, M.D., Chiel, H., Hegemann, P., Landmesser, L.T., and Herlitze, S. (2005). Fast noninvasive activation and inhibition of neural and network activity by vertebrate rhodopsin and green algae channelrhodopsin. Proc. Natl. Acad. Sci. USA *102*, 17816–17821.

Livak, K.J., and Schmittgen, T.D. (2001). Analysis of relative gene expression data using real-time quantitative PCR and the 2(-Delta Delta C(T)) Method. Methods. *25*, 402–408.

Mark, M.D., Ruppersberg, J.P., and Herlitze, S. (2000a). Regulation of GIRK channel deactivation by Galpha(q) and Galpha(i/o) pathways. Neuropharmacology *39*, 2360–2373.

Mark, M.D., Wittemann, S., and Herlitze, S. (2000b). G protein modulation of recombinant P/Q-type Ca^{2+} channels by regulators of G protein signalling proteins. J. Physiol. *528*, 65–77.

Morgan, A., Burgoyne, R.D., Barclay, J.W., Craig, T.J., Prescott, G.R., Ciufo, L.F., Evans, G.J., and Graham, M.E. (2005). Regulation of exocytosis by protein kinase C. Biochem. Soc. Trans. *33*, 1341–1344.

Mosbacher, J., Maier, R., Fakler, B., Glatz, A., Crespo, J., and Bilbe, G. (1998). P_2Y receptor subtypes differentially couple to inwardly-rectifying potassium channels. FEBS Lett. *436*, 104–110.

Nagy, G., Reim, K., Matti, U., Brose, N., Binz, T., Rettig, J., Neher, E., and Sorensen, J.B. (2004). Regulation of releasable vesicle pool sizes by protein kinase A-dependent phosphorylation of SNAP-25. Neuron *41*, 417–429.

Oliveira-Dos-Santos, A.J., Matsumoto, G., Snow, B.E., Bai, D., Houston, F.P., Whishaw, I.Q., Mariathasan, S., Sasaki, T., Wakeham, A., Ohashi, P.S., et al. (2000). Regulation of T cell activation, anxiety, and male aggression by RGS2. Proc. Natl. Acad. Sci. USA *97*, 12272–12277.

Park, M., Penick, E.C., Edwards, J.G., Kauer, J.A., and Ehlers, M.D. (2004). Recycling endosomes supply AMPA receptors for LTP. Science *305*, 1972–1975.

Posner, B.A., Mukhopadhyay, S., Tesmer, J.J., Gilman, A.G., and Ross, E.M. (1999). Modulation of the affinity and selectivity of RGS protein interaction with $G\alpha$ subunits by a conserved asparagine/serine residue. Biochemistry *38*, 7773–7779.

Rhee, J.S., Betz, A., Pyott, S., Reim, K., Varoqueaux, F., Augustin, I., Hesse, D., Sudhof, T.C., Takahashi, M., Rosenmund, C., and Brose, N. (2002). β phorbol ester- and diacylglycerol-induced augmentation of transmitter release is mediated by Munc13s and not by PKCs. Cell *108*, 121–133.

Rosenmund, C., and Stevens, C.F. (1996). Definition of the readily releasable pool of vesicles at hippocampal synapses. Neuron *16*, 1197–1207.

Sakaba, T., and Neher, E. (2003). Direct modulation of synaptic vesicle priming by GABA(B) receptor activation at a glutamatergic synapse. Nature *424*, 775–778.

Saugstad, J.A., Segerson, T.P., and Westbrook, G.L. (1996). Metabotropic glutamate receptors activate GIRK channels in Xenopus oocytes. J. Neurosci. *16*, 5979–5985.

Schaeren-Wiemers, N., and Gerfin-Moser, A. (1993). A single protocol to detect transcripts of various types and expression levels in neural tissue and cultured cells: in situ hybridization using digoxigenin-labelled cRNA probes. Histochemistry *100*, 431–440.

Seifert, R., and Wenzel-Seifert, K. (2002). Constitutive activity of G-protein-coupled receptors: cause of disease and common property of wild-type receptors. Naunyn Schmiedebergs Arch. Pharmacol. *366*, 381–416.

Stauffer, T.P., Ahn, S., and Meyer, T. (1998). Receptor-induced transient reduction in plasma membrane $PtdIns_{(4,5)}P_2$ concentration monitored in living cells. Curr. Biol. *8*, 343–346.

Stevens, C.F. (2004). Presynaptic function. Curr. Opin. Neurobiol. *14*, 341–345.

Takasaki, J., Saito, T., Taniguchi, M., Kawasaki, T., Moritani, Y., Hayashi, K., and Kobori, M. (2004). A novel $G\alpha q$/11-selective inhibitor. J. Biol. Chem. *279*, 47438–47445.

Tang, K.M., Wang, G.R., Lu, P., Karas, R.H., Aronovitz, M., Heximer, S.P., Kaltenbronn, K.M., Blumer, K.J., Siderovski, D.P., Zhu, Y., and Mendelsohn, M.E. (2003). Regulator of G-protein signaling-2 mediates vascular smooth muscle relaxation and blood pressure. Nat. Med. *9*, 1506–1512.

Thomson, A.M. (2000). Facilitation, augmentation and potentiation at central synapses. Trends Neurosci. *23*, 305–312.

Wang, X., Huang, G., Luo, X., Penninger, J.M., and Muallem, S. (2004). Role of regulator of G protein signaling 2 (RGS2) in Ca^{2+} oscillations and adaptation of Ca^{2+} signaling to reduce excitability of RGS2−/− cells. J. Biol. Chem. *279*, 41642–41649.

Wittemann, S., Mark, M.D., Rettig, J., and Herlitze, S. (2000). Synaptic localization and presynaptic function of Ca^{2+} channel β_4-subunits in cultured hippocampal neurons. J. Biol. Chem. *275*, 37807–37814.

Yalcin, B., Willis-Owen, S.A., Fullerton, J., Meesaq, A., Deacon, R.M., Rawlins, J.N., Copley, R.R., Morris, A.P., Flint, J., and Mott, R. (2004). Genetic dissection of a behavioral quantitative trait locus shows that Rgs2 modulates anxiety in mice. Nat. Genet. *36*, 1197–1202.

Young, S.M., Jr. (2005). Proteolysis of SNARE proteins alters facilitation and depression in a specific way. Proc. Natl. Acad. Sci. USA *102*, 2614–2619.

Zamponi, G.W., and Snutch, T.P. (1998). Decay of prepulse facilitation of N type Ca^{2+} channels during G protein inhibition is consistent with binding of a single $G\beta$ subunit. Proc. Natl. Acad. Sci. USA *95*, 4035–4039.

Zerangue, N., and Jan, L.Y. (1998). G-protein signaling: fine-tuning signaling kinetics. Curr. Biol. *8*, R313–R316.

Zucker, R.S. (1999). Ca^{2+}- and activity-dependent synaptic plasticity. Curr. Opin. Neurobiol. *9*, 305–313.